



Geophysical Research Letters

RESEARCH LETTER

10.1029/2019GL085661

Key Points:

- We describe the process for the formation of current sheets and occurrence of reconnection in the quasi-parallel shocked magnetosheath
- The downstream current sheets are formed after the upstream waves penetrate through the shock and are then compressed
- The evidences of reconnection in the downstream include the formation of flux ropes and high-speed flows in the outflow region

Correspondence to:

Q. Lu,
qmlu@ustc.edu.cn

Citation:

Lu, Q., Wang, H., Wang, X., Lu, S., Wang, R., Gao, X., & Wang, S., (2020). Turbulence-driven magnetic reconnection in the magnetosheath downstream of a quasi-parallel shock: A three-dimensional global hybrid simulation. *Geophysical Research Letters*, 47, e2019GL085661. <https://doi.org/10.1029/2019GL085661>

Received 4 OCT 2019

Accepted 10 NOV 2019

Accepted article online 8 JAN 2020

Turbulence-Driven Magnetic Reconnection in the Magnetosheath Downstream of a Quasi-Parallel Shock: A Three-Dimensional Global Hybrid Simulation

Quanming Lu^{1,2}, Huanyu Wang^{1,2}, Xueyi Wang³, San Lu⁴, Rongsheng Wang^{1,2}, Xinliang Gao^{1,2}, and Shui Wang^{1,2}

¹CAS Key Lab of Geospace Environment, School of Earth and Space Sciences, University of Science and Technology of China, Hefei, China, ²CAS Center for Excellence in Comparative Planetology, Hefei, China, ³Physics Department, Auburn University, Auburn, AL, USA, ⁴Department of Earth, Planetary, and Space Sciences, and Institute of Geophysics and Planetary Physics, University of California, Los Angeles, CA, USA

Abstract Satellite observations with high-resolution measurements have demonstrated the existence of intermittent current sheets and occurrence of magnetic reconnection in a quasi-parallel magnetosheath behind the terrestrial bow shock. In this letter, by performing a three-dimensional global hybrid simulation, we investigated the characteristics of the quasi-parallel magnetosheath of the bow shock, which is formed due to the interaction of the solar wind with the Earth's magnetosphere. Current sheets with widths of several ion inertial lengths are found to be produced in the magnetosheath after the upstream large-amplitude electromagnetic waves penetrate through the shock and are then compressed in the downstream. Magnetic reconnection consequently occurs in these current sheets, where high-speed ion flow jets are identified in the outflow region. Simultaneously, flux ropes with the extension (along the y direction) of about several Earth's radii are also observed. Our simulation shed new insight on the mechanism for the occurrence of magnetic reconnection in the quasi-parallel shocked magnetosheath.

Plain Language Summary Benefited from the high-resolution measurements provided by Cluster and Magnetospheric Multiscale missions, there are abundant evidences demonstrating the existence of intermittent current sheets in the terrestrial magnetosheath downstream of a quasi-parallel shock, where magnetic reconnection can occur. However, the process for the formation of these current sheets and occurrence of magnetic reconnection is still unknown. In this letter, the interaction between the high-speed solar wind and the terrestrial magnetosphere is studied with the help of a three-dimensional global hybrid simulation. The bow shock is found to be formed in front of the magnetosphere, and in the subsolar and north parts of the bow shock, the shock is quasi-parallel. In the upstream of the quasi-parallel shock, there exists plenty of large-amplitude low-frequency electromagnetic waves that are convected toward the shock by the solar wind. These waves then penetrate through the shock, and at last current sheets with widths of about several ion inertial lengths are formed in the downstream after these waves are highly compressed by the shock. There are strong evidences supporting the occurrence of magnetic reconnection in these current sheets: the generation of flux ropes, the existence of the reconnection electric field and energy dissipation around the X line, and high-speed plasma flow in the outflow region. The flux ropes have a helical structure of magnetic field lines, and their extension along the y direction is about several Earth's radii.

1. Introduction

The magnetosheath, which is full of turbulent plasmas, is formed behind the bow shock after the high-speed solar wind interacts with the Earth's magnetosphere. When the shock is quasi-perpendicular (the angle between the shock normal direction and upstream magnetic field $\theta_{Bn} > 45^\circ$), the shocked magnetosheath is dominated by ion cyclotron waves and mirror waves that are excited by an ion temperature anisotropy (e.g., Hao et al., 2014; Lee et al., 1986; Lu & Wang, 2006; McKean et al., 1992; Winske & Quest, 1988). However, the characteristics of the magnetosheath behind the quasi-parallel shock ($\theta_{Bn} < 45^\circ$) is still unclear.

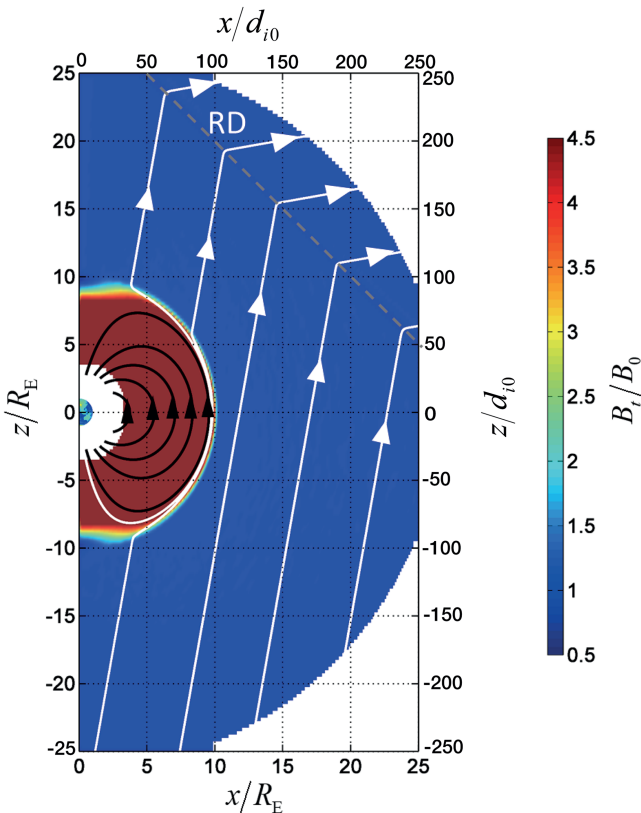


Figure 1. The initial distribution of the magnetic field B_t in the meridian plane. The dashed line denotes the position of the RD. The white and black lines represent the magnetic field lines.

Recently, with the high-resolution measurements of plasma data provided by Cluster and Magnetospheric Multiscale (MMS) missions, intermittent current sheets with widths at ion-electron scales as well as magnetic reconnection have been identified in the magnetosheath downstream of quasi-parallel shocks (Phan et al., 2018; Retinò et al., 2007; Vörös et al., 2017; Yordanova et al., 2016). With Cluster observations, Retinò et al. (2007) identified electromagnetic signatures of magnetic reconnection in the turbulent magnetosheath downstream of a quasi-parallel terrestrial shock. These current sheets are formed due to the existence of large amplitude fluctuations in magnetic field and density and then initiate magnetic reconnection. Magnetic reconnection in the quasi-parallel shock magnetosheath has also been observed by MMS mission (Vörös et al., 2017; Yordanova et al., 2016), and its size can even be down to the electron scale without ion coupling (Phan et al., 2018). Such kind of magnetic reconnection offers a pathway to dissipate magnetic energy to plasma kinetic energy, which subsequently heat and accelerate particles in the magnetosheath.

Although numerous satellite observations have indicated that turbulence-driven reconnection is a ubiquitous process in the quasi-parallel shocked magnetosheath, very few simulations have been performed to study such a process. By performing a two-dimensional global hybrid simulation, Karimabadi et al. (2014) found the presence of magnetic islands in the quasi-parallel shocked magnetosheath, which are considered to be generated due to magnetic reconnection. In this letter, with a three-dimensional (3-D) global hybrid simulation model, we investigate the interactions of the high-speed solar wind with the Earth's magnetosphere and the formation of current sheets in the downstream of the quasi-parallel shock, where magnetic reconnection consequently occurs and flux ropes are generated.

2. Simulation Model

In hybrid simulations, ions are treated as particles, while electrons are considered as a massless and charge-neutralizing fluid. In this letter, a 3-D global hybrid simulation model is used to study the characteristics of the magnetosheath downstream of a quasi-parallel shock. The details of the model can be referred to Lin and Wang (2005), and here only a brief introduction is described. A spherical coordinate system (r , θ , and ϕ) is employed in the simulation model, and the simulation domain covers the dayside region with the geocentric distance $4R_E \leq r \leq 27R_E$ (where R_E is the Earth's radius) and azimuth angle $90^\circ < \phi < 270^\circ$, and the Earth is located at the origin $r = 0$. The electron fluid is assumed to be isothermal in our hybrid simulation model. Initially, the uniform solar wind in $r > 10R_E$ interacts with the Earth's dipole magnetic field limited to $r \leq 10R_E$. Then, the bow shock, magnetosheath, and magnetopause are formed self-consistently on the dayside. In the simulation, the magnetic field and density are normalized by the corresponding values (B_0 and n_0) in the solar wind. The time and length are expressed in the units of the inverse of ion gyrofrequency $\Omega_{i0}^{-1} = eB_0/m_i$ and ion inertial length $d_{i0} = c/\omega_{pi0}$ (where $\omega_{pi0} = (n_0e^2/m_i\varepsilon_0)^{1/2}$ is ion plasma frequency) in the solar wind, respectively. The velocity is scaled to the Alfvén speed $V_{A0} = B_0/\sqrt{\mu_0 m_i n_0}$ in the solar wind. In order to save computational cost, we choose $R_E = 10d_{i0}$. This means that the radius of the Earth in our simulation is about 5 times smaller than that of the real Earth, if we choose a typical interplanetary magnetic field $B_0 = 10nT$ and density $n_0 = 6 \text{ cm}^{-3}$ in the solar wind. There are total $N_r \times N_\phi \times N_\theta = 260 \times 120 \times 140$ grids in the simulation, and nonuniform grids are used in the r direction with a smaller grid size of $\Delta r = 0.5d_{i0}$ around the shock, which is limited to $8R_E \leq r \leq 14R_E$. There are 150–500 particles in each grid cell. The time step is $\Omega_{i0}\Delta t = 0.05$.

For convenience, we present the simulation results in the geocentric solar magnetospheric coordinate system. The solar wind flows into the system along the $-x$ direction from the boundary at $r = 27R_E$, and

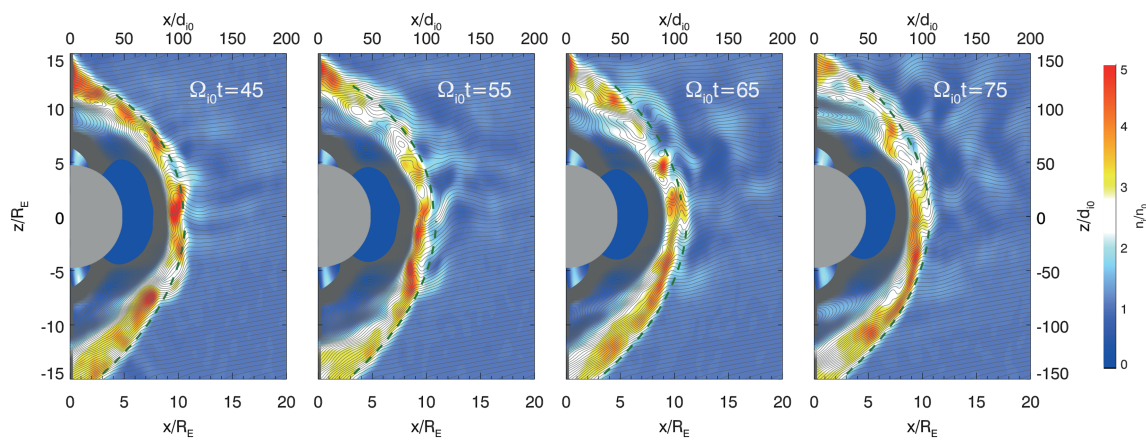


Figure 2. The distribution of the plasma density n in the meridian plane at $\Omega_{i0}t = 45, 55, 65$, and 75 . The magnetic field lines are also superposed in the figure with the black lines, and the green dashed lines represent positions of the bow shock.

outflow boundary conditions are applied at the tailward boundary at $x = 0$. A perfect conducting inner boundary is used at $r = 4R_E$, and the inner magnetosphere with $r \leq 7R_E$ is dominated by a cold ion fluid. The ion and electron plasma beta in the solar wind is $\beta_i = \beta_e = 0.5$, and the Alfvén Mach number is $M_A = 8.83$. As shown in Figure 1, which plots the initial distribution of the magnetic field in the x - z plane, there is a rotational discontinuity (RD) in the solar wind. The RD crosses the point $(30R_E, 0)$ and has an oblique angle of 45° relative to the x direction. The existence of the RD can separate the magnetic field in the solar wind from the Earth's magnetic field. The width of the RD is $0.5d_{i0}$. According to the Rankin-Hugoniot relation, the propagation velocity of the RD is $(u_{RD_x}, u_{RD_y}, u_{RD_z}) = (-9.0, 0.0, -0.98V_{A0})$. Across the RD, the angle between the interplanetary magnetic field and the z direction changes from

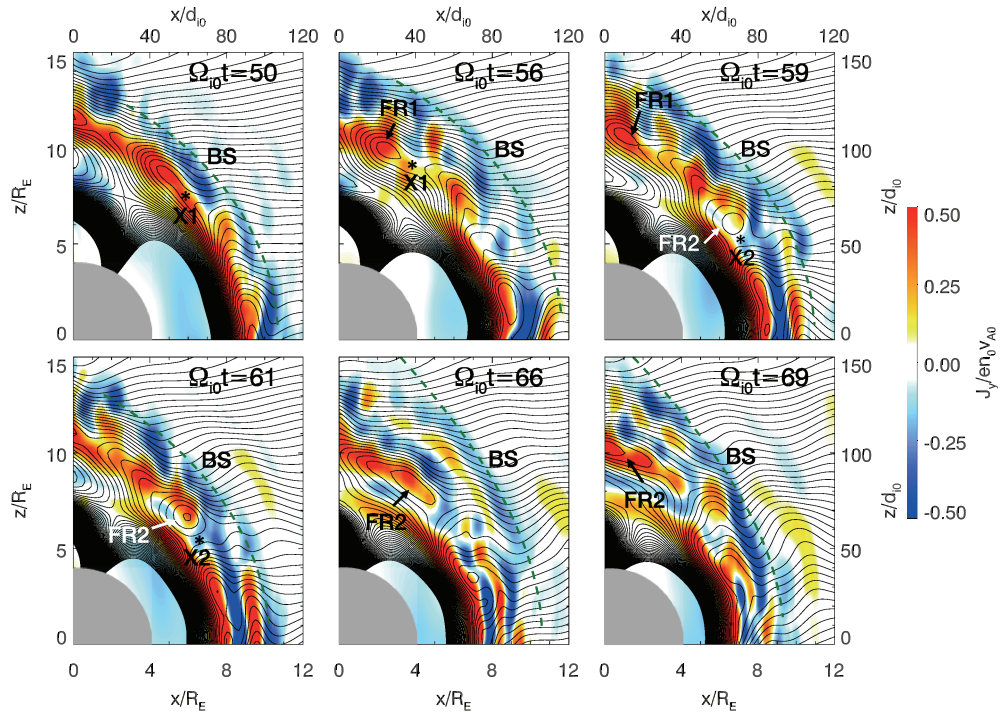


Figure 3. The distribution of the current density J_y in the meridian plane at $\Omega_{i0}t = 50, 56, 59, 61, 66$, and 69 . The magnetic field lines are also superposed in the figure with the black lines, and the green dashed lines represent positions of the bow shock. X1 and X2 denote the positions of the X line, while FR1 and FR2 denote the position of flux ropes.

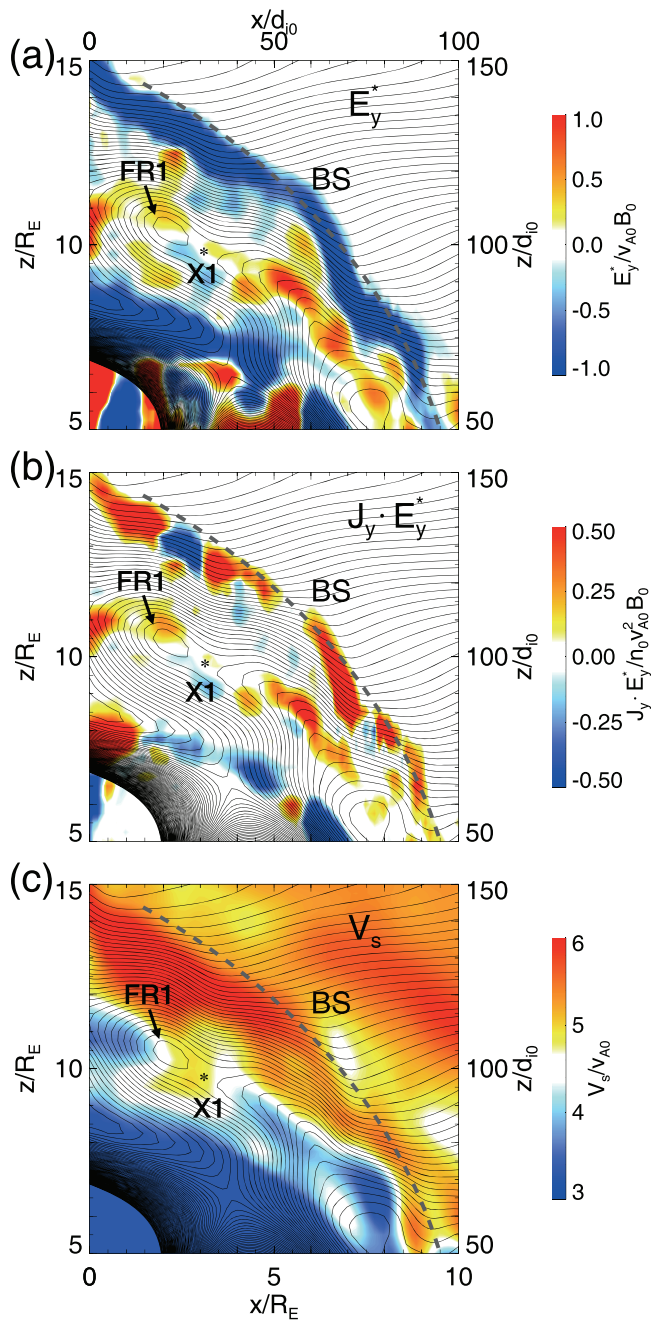


Figure 4. The enlarged view of the structures around the X1 line in the meridian plane at $\Omega_{i0}t = 58$. Here (a), (b), and (c) correspond to the electric field $E_y^* = E_y - (\mathbf{V}_i \times \mathbf{B})_y$, $E_y^* J_y$ and V_s , respectively. The velocity V_s is the ion flow velocity projected to the outflow direction. The magnetic field lines are also superposed in the figure with the black lines, and the grey dashed lines represent positions of the bow shock. At that time, the X1 line is located at $(x, z) = (3.2, 9.8)R_E$.

10° to 80°, and the velocity of solar wind ($u_{IMF_x}, u_{IMF_y}, u_{IMF_z}$) changes from $(-8.83, 0.0, 0.0)V_{A0}$ to $(-8.02, 0.0, -0.81)V_{A0}$.

3. Simulation Results

The bow shock is formed in front of the Earth's magnetosphere at about $\Omega_{i0}t = 10$ due to the interaction between the high-speed solar wind and Earth's magnetosphere, and the shock is quasi-perpendicular at this time. At about $\Omega_{i0}t = 12$, the RD begins to interact with the bow shock, and it completely enters the downstream at $\Omega_{i0}t = 35$. Then, the bow shock becomes quasi-parallel in the subsolar region and north part, while in the south part the bow shock is quasi-perpendicular. In this letter we are only interested in the downstream of the quasi-parallel shock. Figure 2 shows the magnetic field lines and plasma density n in the meridian plane at $\Omega_{i0}t = 55, 65$, and 75 . The RD leaves the tailward boundary at about $\Omega_{i0}t = 40$. Therefore, at these times the quasi-parallel shock is well formed, and the influence of the RD on the downstream characteristics can be neglected. The geocentric distance of the shock is about $10R_E$ at the subsolar point and $15R_E$ at the high altitude. Across the shock, the plasma density is enhanced about 2.5–5 times. In the upstream of the shock, there exist large-amplitude low-frequency waves that are generally considered to be excited by the reflected ions at the shock (e.g., Scholer, 1990; Su et al., 2012; Hao et al., 2016; Liu et al., 2019). In the downstream, several flux ropes with sizes several d_{i0} are formed, and the plasma density is enhanced inside most of these flux ropes.

In order to understand the generation mechanism of these flux ropes in the magnetosheath, we trace the evolution of several typical flux ropes in the magnetosheath. Figure 3 plots the magnetic field lines and current density along the y direction J_y in the meridian plane at $\Omega_{i0}t = 50, 56, 59, 61, 66$, and 69 . After the upstream waves cross the shock, they are compressed and current sheets with widths of $1\text{--}1.5R_E$ (about $10\text{--}15d_{i0}$) are formed in the downstream. Magnetic reconnection occurs in these current sheets. From the figure, we can find that an X line (denoted by X1 in the figure) is firstly formed at about $\Omega_{i0}t = 50$ around $(x, z) = (5.9, 7.8)R_E$ due to magnetic reconnection, and a flux rope (denoted by FR1 in the figure) with the size about $10d_{i0}$ begins to be generated on the upper side of the X1 line. The FR1 flux rope then moves toward the high altitude until it leaves the simulation domain at about $\Omega_{i0}t = 62$. At about $\Omega_{i0}t = 57$, another X line (denoted by X2 in the figure) begins to appear around $(x, z) = (7.1, 5.3)R_E$, and a new flux rope (denoted by FR2 in the figure) is generated on the upper side of the X2 line. The FR2 flux rope also moves toward the high altitude and leaves the simulation domain at about $\Omega_{i0}t = 70$.

Figure 4 exhibits the enlarged view of the structures around the X1 line in the meridian plane at $\Omega_{i0}t = 58$, and at that time the X1 line is located at $(x, z) = (3.2, 9.8)R_E$. Figures 4a–4c correspond to the electric field $E_y^* = E_y - (\mathbf{V}_i \times \mathbf{B})_y$, $E_y^* J_y$, and V_s , respectively. Here V_s is the ion flow velocity projected to the outflow direction. The outflow direction, which can be estimated by the minimum variance analysis method around the X1 line. We can find that there exists a positive value of the electric field E_y^* and $E_y^* J_y$ around the X1 line, where the magnetic energy can be converted into plasma kinetic energy. Because in our hybrid simulation model the electron fluid is assumed to be isothermal, there is no electron off-diagonal pressure tensor term to support the reconnection

estimated by the minimum variance analysis method around the X1 line. We can find that there exists a positive value of the electric field E_y^* and $E_y^* J_y$ around the X1 line, where the magnetic energy can be converted into plasma kinetic energy. Because in our hybrid simulation model the electron fluid is assumed to be isothermal, there is no electron off-diagonal pressure tensor term to support the reconnection

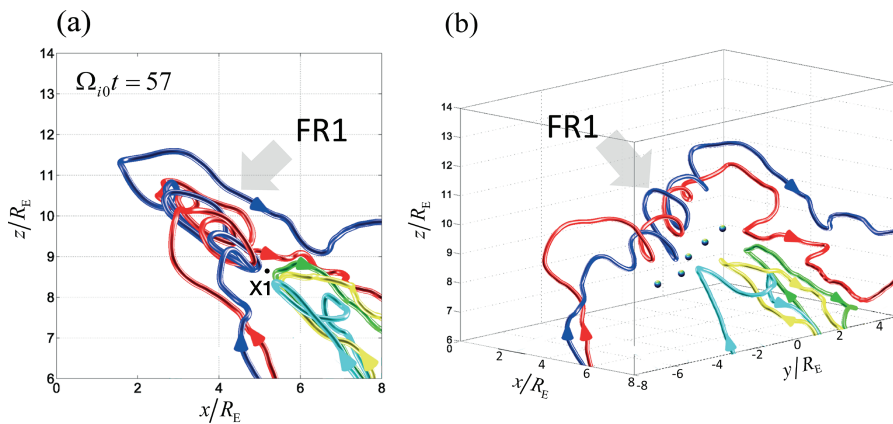


Figure 5. The structure of magnetic field lines around the X1 line at $\Omega_{i0}t = 57$. Here (a) is the projection of the magnetic field lines in the meridian plane, and (b) is the 3-D structure of the magnetic field lines. The X1 line is located at $(x, z) = (5.2, 8.7)R_E$ in the meridian plane.

electric field in the vicinity of the X line (Lu et al., 2015). We can find the obvious existence of E_y^* and $E_y^*J_y$ in the vicinity of the X1 line. At the same time, the X1 line moves to the high altitude in the direction of ambient ion sheath flow with the velocity about $4.4V_{A0}$. On the upper-left side of the X1 line, the velocity V_s is larger than the moving velocity of the X1 line, while it is smaller than the moving velocity of the X1 line in the lower-right side. Therefore, there exists a high-speed plasma flow away from the X1 line in the outflow region, and the speed is about $0.7V_{A0}$. All these evidences are consistent with the occurrence of magnetic reconnection (e.g. Birn et al., 2001, Fu et al., 2006, Wang et al., 2010, 2016).

The 3-D structure of magnetic field lines around the X1 line at $\Omega_{i0}t = 57$ is shown in Figure 5, and at this time the X1 line is located at $(x, z) = (5.2, 8.7)R_E$ in the meridian plane. Figure 5a plots the projection of the magnetic field lines in the meridian plane, while Figure 5b exhibits the 3-D structure of the magnetic field lines. In the meridian plane, there is a flux rope in the upper-left side of the X1 line. The extension of both the X1 line and flux rope along the y direction is about $7R_E$ or $70d_{i0}$, and a helical structure of the magnetic field lines can be easily identified inside the flux rope. We have also examined the extension of other X lines and flux ropes along the y direction, which are about $5\text{--}8R_E$.

4. Conclusions and Discussion

In this letter, we use a 3-D global hybrid simulation to study the interaction between the high-speed solar wind and the terrestrial magnetosphere, and the bow shock is formed in front of the magnetosphere. In the upstream of the quasi-parallel part of the bow shock, there exist large-amplitude low-frequency electromagnetic waves. These waves will move toward and then penetrate through the shock. At last, these waves are compressed to form current sheets in the magnetosheath. Magnetic reconnection occurs in these current sheets, and high-speed plasma flow is observed in the outflow region. Flux ropes with scales about several ion inertial lengths are also generated in these currents sheets. These flux ropes have a helical structure of magnetic field lines, and their extension along the y direction is about $5\text{--}8R_E$. In our hybrid simulation model, electrons are treated as a massless fluid, and electron dynamics is neglected. Due to this limitation, it cannot resolve electron-scale reconnection, which was recently observed by the MMS mission (Phan et al., 2018). Both the formed current sheets and magnetic reconnection in our simulation have an ion-scale size.

Gingell et al. (2017) and Bessho et al. (2019) have also studied the occurrence of magnetic reconnection in a quasi-parallel shock using two-dimensional local kinetic simulations. In their simulations, magnetic reconnection occurs in the shock transition region, and the current sheets are formed due to the interaction between the large amplitude magnetic fluctuations with rippled shock front. However, in our simulation, the current sheets are formed due to the compression of large-amplitude low-frequency electromagnetic waves in the quasi-parallel shocked magnetosheath behind the bow shock. Magnetic reconnection can also be induced in the downstream of the bow shock when the current sheets in the solar wind cross the shock

and are then compressed (Lin, 1997; Phan et al., 2007; Omidi et al., 2009; Guo et al., 2018). However, it is also different from that in our simulation, where magnetic reconnection occurs in the downstream current sheets formed after the excited large-amplitude low-frequency electromagnetic waves cross the shock.

In our simulation, in order to save computational cost, a reduced Earth's radius is used. It is easy to infer that with the increase of the Earth's radius, the quasi-parallel shocked magnetosheath can contain more current sheets. Magnetic reconnection, therefore, should be easier to occur in the magnetosheath.

Acknowledgments

This work was supported by the NSFC Grants 41774169, 41527804, and 41804159 and Key Research Program of Frontier Sciences, CAS (QYZDJ-SSW-DQC010). All simulation data are archived in <http://doi.org/10.4121/uuid:8b17d9fd-fd71-4a49-bc31-9856402efddb>.

References

- Bessho, N., Chen, L. J., Wang, S., Hesse, M., & Wilson, L. B. III (2019). Magnetic reconnection in a quasi-parallel shock: Two-dimensional local particle-in-cell simulation. *Geophysical Research Letters*, 46, 9352–9361. <https://doi.org/10.1029/2019GL083397>
- Birn, J., Drake, J. F., Shay, M. A., Rogers, B. N., Denton, R. E., Hesse, M., et al. (2001). Geospace Environmental Modeling (GEM) magnetic reconnection challenge. *Journal of Geophysical Research: Space Physics*, 106(A3), 3715–3719. <https://doi.org/10.1029/1999JA900449>
- Fu, X. R., Lu, Q. M., & Wang, S. (2006). The process of electron acceleration during collisionless magnetic reconnection. *Physics of Plasmas*, 13(1), 012309. <https://doi.org/10.1063/1.2164808>
- Gingell, I., Schwartz, S. J., Burgess, D., Johlander, A., Russell, C. T., Burch, J. L., et al. (2017). MMS observations and hybrid simulations of surface ripples at a marginally quasi-parallel shock. *Journal of Geophysical Research: Space Physics*, 122, 11,003–11,017. <https://doi.org/10.1002/2017JA024538>
- Guo, Z., Lin, Y., Wang, X., & Du, A. (2018). Magnetosheath reconnection before magnetopause reconnection driven by interplanetary tangential discontinuity: A three-dimensional global hybrid simulation with oblique interplanetary magnetic field. *Journal of Geophysical Research: Space Physics*, 123, 9169–9186. <https://doi.org/10.1029/2018JA025679>
- Hao, Y. F., Lu, Q. M., Gao, X. L., Huang, C., Lu, S., Shan, L. C., & Wang, S. (2014). He⁺ dynamics and ion cyclotron waves in the downstream of quasi-perpendicular shocks: 2-D hybrid simulations. *Journal of Geophysical Research: Space Physics*, 119, 3225–3236. <https://doi.org/10.1002/2013JA019717>
- Hao, Y. F., Lu, Q. M., Gao, X. L., & Wang, S. (2016). Ion dynamics at a rippled quasi-parallel shock: 2D hybrid simulations. *The Astrophysical Journal*, 823(1), 7. <https://doi.org/10.3847/0004-637X/823/1/7>
- Karimabadi, H., Roytershteyn, V., Vu, H. X., Omelchenko, Y. A., Scudder, J., Daughton, W., et al. (2014). The link between shocks, turbulence, and magnetic reconnection in collisionless plasmas. *Physics of Plasmas*, 21(6), 062308. <https://doi.org/10.1063/1.4882875>
- Lee, L. C., Price, C. P., & Wu, C. S. (1986). A study of mirror waves generated downstream of a quasi-perpendicular shock. *Journal of Geophysical Research*, 93, 247–250.
- Lin, Y. (1997). Generation of anomalous flows near the bow shock by its interaction with interplanetary discontinuities. *Journal of Geophysical Research*, 102, 24,265–24,281.
- Lin, Y., & Wang, X. Y. (2005). Three-dimensional global hybrid simulation of dayside dynamics associated with the quasi-parallel bow shock. *Journal of Geophysical Research*, 110, A12216. <https://doi.org/10.1029/2005JA011243>
- Liu, T. Z., Hietala, H., Angelopoulos, V., Omelchenko, Y., Roytershteyn, V., & Vainio, R. (2019). THEMIS observations of particle acceleration by a magnetosheath jet-driven bow wave. *Geophysical Research Letters*, 46, 7929–7936. <https://doi.org/10.1029/2019GL082614>
- Lu, Q. M., & Wang, S. (2006). Electromagnetic waves downstream of quasi-perpendicular shocks. *Journal of Geophysical Research*, 111, A05204. <https://doi.org/10.1029/2005JA011319>
- Lu, S., Lu, Q., Lin, Y., Wang, X., Ge, Y., Wang, R., et al. (2015). Dipolarization fronts as earthward propagating flux ropes: A three-dimensional global hybrid simulation. *Journal of Geophysical Research: Space Physics*, 120, 6286–6300. <https://doi.org/10.1002/2015JA021213>
- McKean, M. E., Winske, D., & Gary, S. P. (1992). Mirror and ion cyclotron anisotropy instabilities in the magnetosheath. *Journal of Geophysical Research*, 97, 19,421–19,432. <https://doi.org/10.1029/92JA01842>
- Omidi, N., Phan, T., & Sibeck, D. G. (2009). Hybrid simulations of magnetic reconnection initiated in the magnetosheath. *Journal of Geophysical Research*, 114, A02222. <https://doi.org/10.1029/2008JA013647>
- Phan, T. D., Eastwood, J. P., Shay, M. A., Drake, J. F., Sonnerup, B. U. Ö., Fujimoto, M., et al. (2018). Electron magnetic reconnection without ion coupling in Earth's turbulent magnetosheath. *Nature*, 557(7704), 202–206. <https://doi.org/10.1038/s41586-018-0091-5>
- Phan, T. D., Paschmann, G., Twitty, C., Mozer, F. S., Gosling, J. T., Eastwood, J. P., et al. (2007). Evidence for magnetic reconnection initiated in the magnetosheath. *Geophysical Research Letters*, 34, L14104. <https://doi.org/10.1029/2007GL030343>
- Retinò, A., Sundkvist, D., Vaivads, A., Mozer, F., André, M., & Owen, C. J. (2007). In situ evidence of magnetic reconnection in turbulent plasma. *Nature Physics*, 3(4), 235–238. <https://doi.org/10.1038/nphys574>
- Scholer, M. (1990). Diffuse ions at a quasi-parallel collisionless shock: Simulations. *Geophysical Research Letters*, 17, 1821–1824.
- Su, Y. Q., Lu, Q. M., Huang, C., Wu, M. Y., Gao, X. L., & Wang, S. (2012). Particle acceleration and generation of diffuse superthermal ions at a quasi-parallel collisionless shock: Hybrid simulations. *Journal of Geophysical Research*, 117(A8), A08107. <https://doi.org/10.1029/2012JA017736>
- Vörös, Z., Yordanova, E., Varsani, A., Genestreti, K. J., Khotyaintsev, Y. V., Li, W., et al. (2017). MMS observation of magnetic reconnection in the turbulent magnetosheath. *Journal of Geophysical Research: Space Physics*, 122, 11,442–11,467. <https://doi.org/10.1002/2017JA024535>
- Wang, R. S., Lu, Q., Nakamura, R., Huang, C., Du, A., Guo, F., et al. (2016). Coalescence of magnetic flux ropes in the ion diffusion region of magnetic reconnection. *Nature Physics*, 12(3), 263–267. <https://doi.org/10.1038/nphys3578>
- Wang, R. S., Lu, Q. M., Du, A. M., & Wang, S. (2010). In situ observations of a secondary magnetic island during collisionless magnetic reconnection and associated energetic electrons. *Physical Review Letters*, 104(17), 175003. <https://doi.org/10.1103/PhysRevLett.104.175003>
- Winske, D., & Quest, K. B. (1988). Magnetic field and density fluctuations at perpendicular supercritical collisionless shocks. *Journal of Geophysical Research*, 93, 9681–9693. <https://doi.org/10.1029/JA093iA09p09681>
- Yordanova, E., Vörös, Z., Varsani, A., Graham, D. B., Norgren, C., Khotyaintsev, Y. V., et al. (2016). Electron scale structures and magnetic reconnection signatures in the turbulent magnetosheath. *Geophysical Research Letters*, 43, 5969–5978. <https://doi.org/10.1002/2016GL069191>